

# Application of Mimosa Pudica Mechanoreceptors to Electronic Skin Design

THESIS

Presented in Partial Fulfillment of the Requirements for graduation *with Honors*  
*Research Distinction* in Electrical and Computer Engineering in the undergraduate  
colleges of The Ohio State University

By

Seth Micah Ringel

The Ohio State University

2015

Undergraduate Honors Thesis Committee:

Dr. Liang Guo, Advisor

Dr. Lee Potter

Copyright by  
Seth Micah Ringel  
2015

## Abstract

Mechanoreceptor cells in *Mimosa Pudica* – a plant known for its rapid leaf movements when touched – can be used as a possible tactile sensor to create a flexible, high-resolution electronic skin. To test the viability of this solution, mechanoreceptor cells have been incorporated into a hydrogel to ensure their mechanosensitive properties are retained after isolation. Gelling agent is used to solidify a culture of the mechanosensitive cells onto a microelectrode array. This allows the monitoring of electrical responses to an applied mechanical stimulus. It is shown that more experimentation must be done in order to prove that these cells do retain their ability to transduce mechanical stimulus into an electrical response, and thus would serve as a viable tool in future electronic skin designs.

Moving forward, calcium imaging will be used to optically characterize the response of the cells in terms of the firing of action potentials upon mechanical stimulation. This will also be used to observe if the cells are in fact firing in response to the stimulus. This will also allow for a specific determination of the cells responsible for the electrical response. Additional tests may be run to test how well the material localizes electrical responses to areas of stimulation by employing multiple channels of the microelectrode array. This simple bio-complex material has the potential to provide the basis for a larger scale, complex electronic skin that may be used in tactile sensing prosthetics, soft robotics, and smart materials.

## Dedication

This document is dedicated to my family, friends, and mentors.

## Acknowledgments

I would like to thank Professor Liang Guo for his assistance and support throughout the duration of this project.

I would like to thank Yongchen Wang for his knowledgeable assistance in formulating the isolation protocol for this project.

I would like to thank the entirety of the Biotronics Lab group for their support and feedback.

This work was supported by The Ohio State University Materials Research Seed Grant Program, funded by the Center for Emergent Materials, an NSF-MRSEC, grant DMR-1420451, the Center for Exploration of Novel Complex Materials, and the Institute for Materials Research. I was also supported by the Undergraduate Education Summer Research Fellowship and the Undergraduate Honors Research Scholarship at OSU.

Vita

May 2011 .....Bexley High School

May 2015 .....B.S. Electrical and Computer Engineering,

Ohio State University

Fields of Study

Major Field: Electrical and Computer Engineering

Minor Field: Neuroscience

## Table of Contents

Abstract .....	ii
Dedication .....	iii
Acknowledgments.....	iv
Vita.....	v
List of Tables .....	viii
List of Figures .....	ix
Chapter 1: Introduction .....	10
1.1 Motivation .....	10
1.2 Background Information .....	11
1.3 Relevant Technologies .....	13
1.4 Unique Advantages of this Scheme .....	15
Chapter 2: Methods.....	16
2.1 Preparing the Enzyme Digestion Solution .....	16
2.2 Isolating the Mechanoreceptor Protoplasts .....	16
2.4 Recording from the Material .....	18
Chapter 3: Results .....	19

3.1 Isolation of Protoplasts.....	19
3.2 Electrophysiological Results.....	20
Chapter 4: Discussion.....	21
Chapter 5: Summary.....	24
5.1 Conclusions.....	24
5.2 Recommendations.....	25
5.2.1 Isolation Procedure.....	25
5.2.2 Gelling of Protoplast Solution.....	25
5.2.3 Electrophysiological Testing.....	25
References.....	27
Appendix A: Pictures.....	29
Appendix B: Code.....	30
Appendix C: Bulk Data.....	34



## List of Tables

Table 1. Human Skin Characteristics and Corresponding Electronic Skin Requirements <sup>[5]</sup>	
.....	11

## List of Figures

Figure 1. Closing Action of <i>Mimosa Pudica</i> .....	12
Figure 2. Stretchable MEA from Langer Lab <sup>[10]</sup> .....	15
Figure 3. FFT and Time Domain Signal of Electrophysiological Recording.....	20
Figure 4. FFT of Filtered Signal .....	21
Figure 5. Ideal Compound Action Potential .....	21
Figure 6. Filtered Time Domain Signal .....	21

## Chapter 1: Introduction

Skin is the largest sensory organ in the human body<sup>[1]</sup>. Acting as our intermediaries with the physical world, various cutaneous sensors allow us to distinguish shapes, textures, pressures, and temperatures by converting physical stimuli into electrical signals that are processed in the somatosensory cortex<sup>[1]</sup>. Electronic skin research is an important field in prosthetics, medicine, and soft robotics with uses in pressure and temperature sensation and monitoring and robotic control. A conventional design process was followed for the creation of a novel pressure sensing mechanism for an electronic skin design. The following sections outline the motivation behind the design and electronic skins in general, a brief review of current technology, and the advantages of the proposed device design.

### *1.1 Motivation*

With approximately 2 million amputees in the United States alone, and an estimated 185,000 new amputees each year<sup>[2]</sup>, there is a significant portion of the population that would benefit from the advancement of electronics skin for prosthetic technology. One of the premier faults of current advances in prosthesis technology is the reliance on visual information as the only source of feedback. Tactile sensing capability, along with proprioception and temperature sensing, are the most vital feedback mechanisms that are not available currently to amputees. The reinstatement of these sensory feedback mechanisms requires the creation of a neural interface and a

comprehensive, high-resolution electronic skin. Additionally, there are approximately 735,000 Americans in assisted living<sup>[3]</sup>. Many current artificial intelligence thrusts are focused on assistive robotic care<sup>[4]</sup>, where precise pressure appliance and spatial and tactile awareness are necessary traits. These highly equipped robots are proposed for use in rescue operations as well<sup>[4]</sup>. Flexible electronic skins following the design proposed in this work, with its potential to conform, stretch, and sense touch and pressure, would provide part of the solution for these people. Table 1 shows one interpretation of some of the necessary qualities for an electronic skin<sup>[5]</sup>.

Parameter	Human Skin	Electronic Skin Requirements
Spatial Resolution	1mm	1-2mm
Temporal Resolution	20-40ms	1-10ms
Working Range	>10kPa	1-1000g
Hysteresis	High	Low

Table 1. Human Skin Characteristics and Corresponding Electronic Skin Requirements<sup>[5]</sup>

### *1.2 Background Information*

Some of the most important attributes for electronic skin are flexibility, spatial tactile resolution, and sensitivity<sup>[4]</sup>. Flexibility allows the material to curve around objects such as fingers or robotic manipulators; resolution allows for fine control through more informed spatial awareness; and sensitivity allows – especially in the case of soft robotics for fine manipulation of objects<sup>[4]</sup>. Thus, high-resolution tactile sensing that does not degrade with deformation is a vital goal for electronic skins. Currently, many common

pressure sensitive materials are stiff and the resulting sensors are generally inflexible<sup>[6]</sup>. As the majority of electronic skin designs incorporate an array of pressure sensitive components on an active matrix back plane, this yields bulky, stiff devices with limited functionality in cases where malleability is an essential quality. Additionally, these devices are dissimilar in many of the mechanical properties of true skin and have generally poor resolution which is limited by the size of each tactile pixel. One of the challenges that current electronic skin research faces is the creation of a microscale-sensing, soft mechano-electrical transducer that can be integrated into large scale electronics.

The *Mimosa Pudica*, or ‘Sensitive Plant’ is known for its rapid leaflet closure when touch, cut, burned, or stimulated electrically (Fig. 1)<sup>[7]</sup>. The mechanism of *Mimosa Pudica* leaf movement has been

investigated since the 18<sup>th</sup> century, but not until very recently were the mechanoreceptor cells responsible for the leaflet movement identified and localized to the tertiary pulvini<sup>[7]</sup>. In this work we aim to validate the use of *Mimosa Pudica* mechanoreceptor cells throughout the pulvini and petiole in a complex electronic skin design by implementing them into a simplified artificial complex material – heretofore referred to as a ‘bio-complex’ material - and characterizing the cells’ electrical responses to

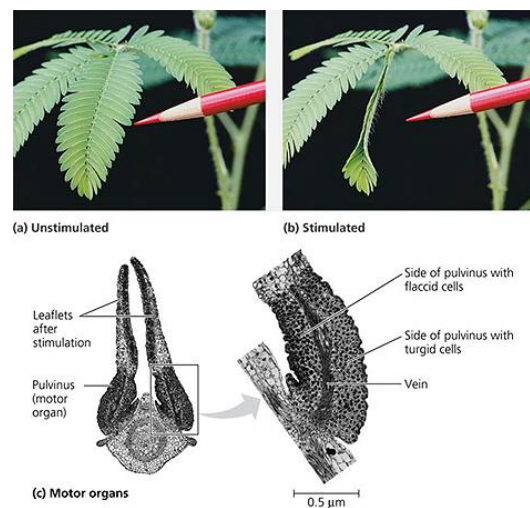


Figure 1. Closing Action of *Mimosa Pudica*

mechanical stimuli. The use of *Mimosa* cells in place of common artificial components yields several important advantages which will be outlined in the following section.

### *1.3 Relevant Technologies*

Most current electronic skins rely on inflexible pressure sensitive components that limit the applicability of the overall device by placing restrictions on the flexibility and texture of the final product<sup>[6]</sup>. The use of mechanosensitive biological cells allows for the creation of a more flexible material, as the cells are small enough to allow the overall material to bend without being damaged. Along similar lines, the small size of the mechanoreceptor cells (~20-50um)<sup>[7]</sup> allows for the potential of very fine tactile resolution. The size of most current tactile pixels ('taxels') range from hundreds of microns to tens of millimeters and is limited by the pressure-sensing components<sup>[8]</sup>. Thus, a material utilizing the *Mimosa* mechanoreceptor cells has the potential for much higher resolution than other technologies and even than standard human skin which reaches maximum spatial resolution of just over 500 microns on the lip and only 1mm on the fingertip<sup>[9]</sup>. The ability to have higher tactile resolution could have significant impact on medical practices in particular through inventions such as tactile-sensing surgical gloves and personal biomedical monitoring devices.

Many common devices use organic field-effect transistors or piezoelectric devices as the mechanosensitive element, which both require significant time and capital, and require lithographic methods for production<sup>[4,5]</sup>. Additionally, piezoelectric materials experience drift in sensor response over time and give unreliable measurements for static

stimuli and are susceptible to changes in temperature which illicit identical responses to tactile stimuli<sup>[4,5]</sup>. Piezoresistive elements are also being explored although they exhibit large hysteresis and are subject to significant variations with temperature that cause responses indistinguishable from that of tactile stimuli<sup>[4,5]</sup>. Capacitive sensors are another technology being explored, although they have an undesirable relationship between pixel size and signal-to-noise ratio that causes inherent limitations on tactile resolution, among other setbacks such as their susceptibility to influence by external interference and their slow response time<sup>[4,5]</sup>. Optical devices using waveguides in flexible substrates are another avenue being explored. However, the significant number of light sources needed for a high resolution of tactile sensing implies significant power consumption relative to other designs and renders this scheme less attractive<sup>[5]</sup>.

Additional materials are being explored, such as carbon nanotubes, for use as the active back plane material<sup>[5]</sup>. The use of carbon nanotubes is attractive for the ease of manufacture in large scales<sup>[5]</sup>. Additionally, they have been proven to show exceptional electrical and mechanical properties<sup>[5]</sup>. However, they have a high price point and are unproven under mechanical strain in a flexible material<sup>[5]</sup>. Graphene films are another attractive option, however, they must be transferred to plastic substrates for use – a process which frequently introduces defects and limits device size<sup>[5]</sup>. Nanowires from ZnO, CdSe, Si, and GaAs are also options for the active matrix material. Although some designs have shown good results, they incur a very large production cost and a significant amount of time to produce<sup>[5]</sup>. Lastly, organic polymers have been explored for this use. These devices have proven very tunable via chemical synthesis and are attractive for their

similarity in mechanical properties to human skin<sup>[5]</sup>. However, their performance has not been shown to approach that of inorganic schemes<sup>[5]</sup>.

#### *1.4 Unique Advantages of this Scheme*

The protocol proposed here calls for an entirely biological pressure sensor that is gelled onto a simple microelectrode array (MEA). The end device proposed by the Guo lab in 2014 calls for the use of a stretchable MEA (sMEA) of the design used in [10] as

the back plane device (Fig. 2). There are numerous advantages of this scheme are that the mechanoreceptor cells incur very little cost and are easily isolated for use.

The fact that the mechanical sensing is entirely self-contained means that the flexibility of the material will not be

negatively impacted by these mechanotransduction elements because of their small size and lack of interconnectedness. Additionally, the procedure of isolation is entirely ‘green,’ and the power requirements of the final device are minimal as the sensing is entirely passive and it is only the signal analysis that requires power.

The mechanoreceptor cells were isolated via enzymatic digestion and incorporated into a simple material composed of gelled culture media and adhered to the surface of an MEA. This simple setup will allow the validation of the claim that these cells may be used in a viable electronic skin design by demonstrating that they retain

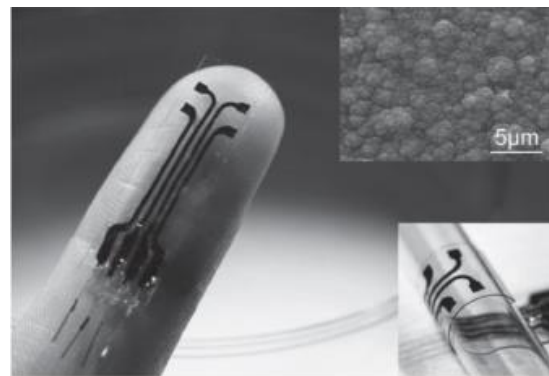


Figure 2. Stretchable MEA from Langer Lab<sup>[10]</sup>



their mechanosensitive properties *in vitro*. This is a preliminary step in the larger project to create a fully coordinated polydimethylsiloxane (PDMS) and hydrogel based electronic skin with incorporated microfluidic structures for cell support and protection.

## Chapter 2: Methods

Mature *Mimosa Pudica* plants were obtained from a supplier. They were watered every other day with 50mL of tap water and kept in an approximate day/ night cycle of 12/12 hours in a  $21\pm 2^{\circ}\text{C}$  controlled climate.

### *2.1 Preparing the Enzyme Digestion Solution*

In a 15mL falcon tube, Cellulase Onozuka R-10 (0.05g), Macerozyme R-10 (0.05g), mannitol (1.25ml), KCl (25ul), and MES (0.25ml) were combined, vortex mixed, and heated for 10 minutes in a  $55^{\circ}\text{C}$  water bath. The mixture was then cooled for 1 minute in an ice bath.  $\text{CaCl}_2$  (25ul) and distilled  $\text{H}_2\text{O}$  (0.95ml) were then added and the solution was vortex mixed.

### *2.2 Isolating the Mechanoreceptor Protoplasts*

A diagram of the *Mimosa Pudica* anatomy may be seen in Fig 1 of Appendix A. One petiole of the plant was cut above the primary pulvinus using microscissors. The attached pinnae were removed below the secondary pulvini and discarded. The petiole, with pulvini at both ends, was then cut into thin slices ( $\sim 500\mu\text{m}$ ) perpendicular to its longitudinal axis using microscissors and immediately placed into 1mL of freshly prepared enzyme solution in a 6.5mm Petri dish.

1µm of both fluo-3 fluorescence protein and 20% pluronic F-127 in DMSO were mixed with 48µm of enzyme solution, vortex mixed, and added back to the enzyme solution. The fluorescence protein serves to illuminate calcium movement for calcium ion imaging. The mixture was then wrapped in aluminum foil to prevent photobleaching of the dye solution. The mixture was then set on a climate controlled ( $37\pm 0.2^{\circ}\text{C}$ ) stirring platform (Thermo Scientific MaxQ 4450) for 1 hour at 50rpm followed by an additional 10 minutes at 100rpm.

An automatic pipette (Eppendorf EasyPet 3) was then used to transfer the mixture to a 15mm Petri dish while pouring through a 40µm filter. The choice of pipette was made because of the large diameter pipette tube openings that allow for the plant matter to be transported along with the solution. The 3.5mm Petri dish was then washed once with 3mL ice-cold W5 solution. The wash solution was then filtered and added to the 15mm Petri dish. The resulting mixture was then transferred to a 15mL Falcon tube for centrifugation. The mixture was centrifuged at 100rpm for 2 minutes, or until a visible pellet formed on the bottom of the tube.

The supernatant solution was then removed and discarded, leaving approximately 50µm of liquid. A gentle swirling resuspended the protoplasts in the remaining solution. At this point, the solution may be observed under a microscope to visually inspect the protoplast yield.

The suspended protoplast solution was then pipetted into the center of a 64-electrode MEA (Multichannel Systems 60MEA500/30iR-Ti). The choice of MEA was made to minimize the expense of the device while still allowing for the needs of future

experimentation, such as the employment of multiple channels for resolution testing. The droplet was positioned such that it covered the electrode leads in the rectangular sensing area of the MEA.

### *2.3 Preparing the Cells for Electrical Recordings*

A molten agar solution (2% w/v) was prepared by using 2mL of W5 solution and 4mg agar powder. The mixture was vortex mixed and warmed in a water bath to 55°C. After the agar solution reached temperature, it was vortex mixed and immediately pipetted around the protoplast droplet circling inward, and finally on top of the droplet. The intention of this method is to solidify the protoplast droplet while keeping the majority of the protoplasts in the center of the MEA.

The agar gelled material was then allowed to solidify onto the device in a ventilation hood for approximately 5 hours, or until the material was completely gelled.

### *2.4 Recording from the Material*

Initial recordings were set up as single channel voltage recordings. The ground pin and one recording electrode on the MEA were connected to the ground pin and voltage-in of one channel of an amplifier (Brownlee Precision Model 440 Instrumentation Amplifier). The internal low-pass filter of the amplifier was varied between 1kHz-20kHz. The internal high-pass filter was varied between 0.1Hz-75Hz. The gain function was varied between 400-5000. The amplifier output was sent to a data acquisition system (NIDAQmx USB 6353) which was connected to a laptop computer

running LabVIEW as the user interface which plotted the data in real time. Two weights (0.1799g and 0.1745g) were used for control, acute, chronic, and set tests. The tests are explained as follows:

- Control test: No weight stimulus was applied – essentially a recording of electrical noise
- Acute test: The weight was dropped from a height of 1cm and removed immediately.
- Chronic test: The weight was dropped from a height of 1cm and allowed to rest on the material for the duration of the recorded experiment
- Set test: The weight was rested on the material in advance of the experiment and allowed to remain for the duration of the recorded experiment.

Each of these tests was run for a total of 15 seconds. 5 second windows containing comprehensive data collected at 1kHz were analyzed. The data from LabVIEW was exported to Microsoft Excel and then read into Matlab for filtering and data analysis.

## Chapter 3: Results

### *3.1 Isolation of Protoplasts*

Isolation of the protoplasts on a large scale was moderately successful. The theoretical yield of the protocol followed is  $1.5 \times 10^5$  cells for the amount of material used. Experimental yield of live cells was calculated to be  $10^4$  by Eq. 1 and a standard microscope image of post-isolation. A 2D yield calculation was appropriate as it was

shown by visual inspection that the vast majority of the cells settled to the bottom plane of the liquid. The droplet area was approximated as the area of the electrode square that it covered.

$$Yield = \frac{\#Cells * Total Area of Droplet}{Area of Image} \quad (1)$$

Although the 10% yield at best is not ideal, it does prove that the cells can be isolated successfully and incorporated in a gel-overlaid device while remaining alive. However, the electrical response of the device was shown to be lacking. The low yield is a probable factor in these results.

### 3.2 Electrophysiological Results

Successful electrophysiological tests would represent the effective transduction of the mechanical stimulus into a series of compound electrical impulses from the *Mimosa* cells embedded into the material. Initial tests were taken at amplifier settings of: high-pass filter at 0.1Hz, low-pass filter at 1kHz, gain factor at 400. Data was sampled at a frequency of 1kHz and graphed in LabVIEW ( Code.B1).

The data was then exported to a Microsoft Excel file where it was read by a Matlab program (Code B2). The results for both the initial isolation and the control experiment taken with these settings showed significant noise in the 60Hz region, most

likely due to the power source (Fig. 3). In order to filter

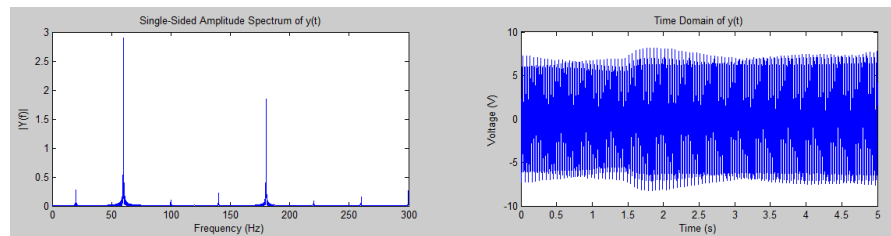


Figure 3. FFT and Time Domain Signal of Electrophysiological Recording

the noise, the signal had to be resampled to a sampling frequency of some multiple of the noise frequency. Thus, the 1kHz sampling frequency was first interpolated by a factor of 6 and then decimated by a factor of 10 to yield an effective sampling rate of 600Hz. Filtering of this data via a 60Hz notching comb filter eliminated the majority of this noise (Fig.4). However, the remainder of the signal did not show any characteristics of a compound action potential. A standard compound action potential would appear as in Fig 5. This process was repeated for each set of collected data and in each case, no significant signal was found and the time domain signal retained the appearance of noise (Fig. 6).

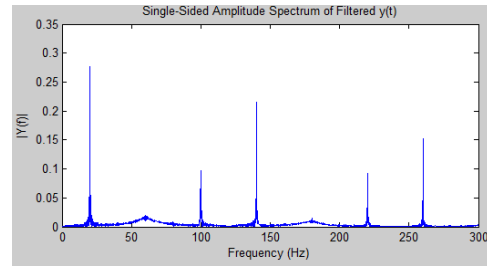


Figure 4. FFT of Filtered Signal



Figure 5. Ideal Compound Action Potential (The McGill Physiology Virtual Lab)

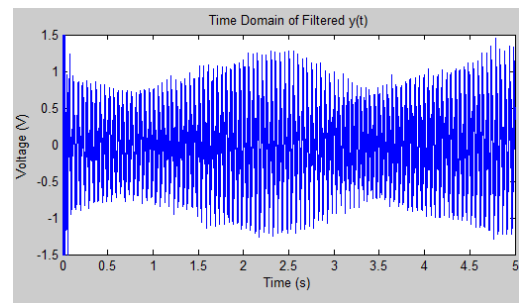


Figure 6. Filtered Time Domain Signal

#### Chapter 4: Discussion

*Mimosa Pudica* has the unique ability to respond to touch stimulus through the function of an action-potential like electrical response mechanism. The purpose of this work is to provide the framework validation of the concept to isolate the cells responsible

for the mechanotransduction of tactile stimulus for use in a tactile-sensing skin.

Successful recording of a useable electrical response from the Mimosa cells would prompt the manufacture of a more complex design proposed in 2014 by the Guo lab. The design includes an sMEA<sup>[10]</sup> fabricated on a PDMS substrate which will serve as both the electrical readout and mechanical support, much as the planar MEA does in this work. An aqueous mixture of the isolated protoplasts and a chosen pre-hydrogel would be poured onto the device and a gelling agent would be added while microfluidic vasculature would be added to improve cell viability via similarity to the *in vivo* environment. The use of a porous hydrogel would also aid in increasing the cell viability *in vitro* via similar biomimetics. A miniaturized pump would be employed to continuously circulate culture medium through the microfluidic channels and complete the design of the vasculature as an artificial representation of human skin. The use of a PDMS substrate implies significant ability of the device to stretch and flex, as well as an inherent biocompatibility<sup>[5]</sup>.

The specific aims of this project were to successfully isolate the aforementioned protoplasts, to gel them successfully into a simple material overlaid on an MEA, and to examine the parameters useful for extracting an electrical signal from data collected in response to a mechanical stimulus.

Several protocols of isolation were explored, with various low yield results. With the aid of Yongchen Wang, a Ph.D. student in the Guo lab, a procedure that was formed by combining a mixture of the protocols from [11] and [12] was found to be successful at

isolating the protoplasts *in vitro* over the course of a few hours with a high yield. The specific details of the isolation are outlined in the Methods section.

Agar gel was used to gel the protoplasts onto the MEA for electrical recording purposes. Several different weight/volume percentages were used within the standard 1-2% w/v range. Agar was chosen as the gelling agent because of its ease of use and availability, as well as its proven record with cell culture<sup>[13]</sup>. Agar powder was mixed with W5 solution to the appropriate percentage and was heated to 55°C and then allowed to cool to its gelling temperature which ranges from 32-40°C. As the gel experiences hysteresis in the gelling process, it withstands heats up to approximately 85°C. In a ventilation hood, gelling time was approximately 5 hours, although it varied with the agar percentage. It is noted that storing the gel mixture after pipetting into the MEA in a 4°C refrigerator is a possible method to accelerate the gelling process without damaging the protoplasts, which can withstand the temperature. It is also suggested that adding the agar powder to boiling water and maintaining the solution at 55°C until use could improve the gelling performance.

The data was collected using an amplifier and data acquisition system connected to a single channel on the MEA. 5 second recordings snippets from LabVIEW during which a stimulus was presented were exported to a Microsoft Excel file where they could be read in Matlab for analysis. Initial analysis of a completed design showed voltage fluctuations at the moment of impact that then settled in approximately 0.5s. The immediate settling and lack of continued fluctuation for chronic tests was suspicious, as an attenuating signal was expected instead of a complete reversion to the unstimulated



signal. This led to the design of a control chip, consisting of gelled W5 solution without any isolated cells overlaid on the MEA to test for similar responses. This experiment yielded very similar results as the initial completed chip experiment. Thus, the initial spike is likely an artifact from the impact and not the result of any electrical response from the embedded cells. The control data, as well as the device data were also analyzed by their Fast Fourier Transforms (FFTs) and showed a significant noise signal at 60Hz. Thus, with the aid of Forest Kunecke, an undergraduate electrical engineering student in the Guo lab, a notching comb filter was designed to filter out the 60Hz signal in Matlab. First the data had to be resampled from the original 1kHz sampling frequency to match a multiple of the 60Hz noise signal. The data was first interpolated by a factor of 6 and then decimated by a factor of 10 for an effective sampling frequency of 60Hz.

## Chapter 5: Summary

### *5.1 Conclusions*

The isolation process of the *Mimosa Pudica* mechanoreceptors was successful for a low yield of material – only approximately 10% of the expected cell density was observed. However, cells were shown to remain viable even after the gelling process. Electrophysiological recordings showed a noisy signal with what is likely a motion artifact in all experimental tests. The data did not show any electrical response of the mechanoreceptor cells to the mechanical stimulus applied in any experimental design scheme after filtering a 60Hz noise signal from the power source. Any eventual product

would have to pass FDA standards of approval for both biocompatibility of the electronic skin and the standards of approval for a nerve interface.

## *5.2 Recommendations*

### *5.2.1 Isolation Procedure*

It was seen throughout the isolation processes that were tested that finer cuts of plant material yielded higher densities of cells in the final isolation. Using a method such as in [11] where a fresh razor is used to mince the plant material could potentially help increase the yield by increasing the surface area available for enzymatic digestion. Additionally, a longer digestion time could be employed.

### *5.2.2 Gelling of Protoplast Solution*

A quicker gelling time and stiffer gel may be employed through several of the methods discussed in the Discussion section of this thesis. These include a higher heating point or the addition of agar powder to already boiling water, the placement of the molten agar and protoplast solution into a refrigerator, and further increasing the agar w/v percentage. However, increasing the percentage of agar in the solution could result in an osmotic imbalance that could be hurtful to the cells vitality.

### *5.2.3 Electrophysiological Testing*

It is probable that several factors affected the lack of response to mechanical stimuli other than the possibility that the protoplasts do not retain their mechanosensitive properties. The cell density, which has been addressed, is likely one. Another possible factor is the stiffness of the gel, which has also been addressed. Other possible factors are

the small force that the stimulus imparted, and the limited number of channels that were recorded from. The former may be addressed by using a heavier weight, however one must be cautious to not injure the MEA device. A thicker layer of agar gel may be helpful in supporting the structure of the device while still transferring more of the impact force. The latter may be addressed by employing more channels for electrophysiological recordings. Thus, any electrical response from a mechanoreceptor cell would be more likely to be recorded.

## References

- [1] F. L. Rice, P. J. Albrecht. (2007) *The Senses: A Comprehensive Reference*. Academic Press, Ch.1.
- [2] Limb Loss Statistics. (2015). Retrieved April 17, 2015, from <http://www.amputee-coalition.org/limb-loss-resource-center/resources-by-topic/limb-loss-statistics/limb-loss-statistics/>
- [3] Resident Profile. (2010). Retrieved April 17, 2015, from <http://www.ahcancal.org/ncal/resources/Pages/ResidentProfile.aspx>
- [4] Chortos, A., & Bao, Z. (2014). Skin-inspired electronic devices. *Materials Today*, 321-331.
- [5] Hammock, M., Chortos, A., Tee, B., Tok, J., & Bao, Z. (2013). 25th Anniversary Article: The Evolution of Electronic Skin (E-Skin): A Brief History, Design Considerations, and Recent Progress. *Advanced Materials*, 5997-6038.
- [6] Jain, Advait, Marc D Killpack, Aaron Edsinger, and Charles C Kemp. 2013. "Reaching in clutter with whole-arm tactile sensing." *The International Journal of Robotics Research* 32 (4):458-482.
- [7] Visnovitz, T., Világi, I., Varró, P., & Kristóf, Z. (2007). Mechanoreceptor Cells on the Tertiary Pulvini of L. *Plant Signaling & Behavior*, 462-466.
- [8] Wu, W., Wen, X., & Wang, Z. (2013). Taxel-Addressable Matrix of Vertical-Nanowire Piezotronic Transistors for Active and Adaptive Tactile Imaging. *Science*, 952-957.
- [9] Boven, R., & Johnson, K. (1994). The limit of tactile spatial resolution in humans: Grating orientation discrimination at the lip, tongue, and finger. *Neurology*, 2361-2361.
- [10] Guo, L., Ma, M., Zhang, N., Langer, R., & Anderson, D. (2014). Stretchable Polymeric Multielectrode Array for Conformal Neural Interfacing. *Advanced Materials*, N/a-N/a.
- [11] Zhai, Z., H. I. Jung, and O. K. Vatamaniuk. 2009. "Isolation of protoplasts from tissues of 14-day-old seedlings of *Arabidopsis thaliana*." *J Vis Exp* (30). doi: 10.3791/1149.

- [12] Yoo, S., Cho, Y., & Sheen, J. (2002). Arabidopsis mesophyll protoplasts: A versatile cell system for transient gene expression analysis. *Nature Protocols*, 1565-1572.
- [13] Babbar, S., Jain, R., & Walia, N. (2005). Guar gum as a gelling agent for plant tissue culture media. *In Vitro Cellular & Developmental Biology - Plant*, 258-261.
- [14] Shu, B., Gong, S., Ma, Z., Yap, L., & Cheng, W. (2014). Mimosa-Inspired Design of Flexible Pressure Sensor with Touch Sensitivity. *Small*.
- [15] Shen, A., Hamlington, B., Knoblauch, M., Peters, W., & Pickard, W. (n.d.). *Forisome Based Mimetic Smart Materials*.
- [16] Knoblauch, M., Noll, G., Müller, T., Prüfer, D., Schneider-Hüther, I., Scharner, D., . . . Peters, W. (2003). Corrigendum: ATP-independent contractile proteins from plants. *Nature Materials*, 353-353.
- [17] Wang, X., Gu, Y., Xiong, Z., Cui, Z., & Zhang, T. (2014). Silk-Molded Flexible, Ultrasensitive, and Highly Stable Electronic Skin for Monitoring Human Physiological Signals. *Advanced Materials*, 1336-1342.
- [18] Nisch, W., Böck, J., Egert, U., Hämmerle, H., & Mohr, A. (1994). A thin film microelectrode array for monitoring extracellular neuronal activity in vitro. *Biosensors and Bioelectronics*, 737-741.

Appendix A: Pictures

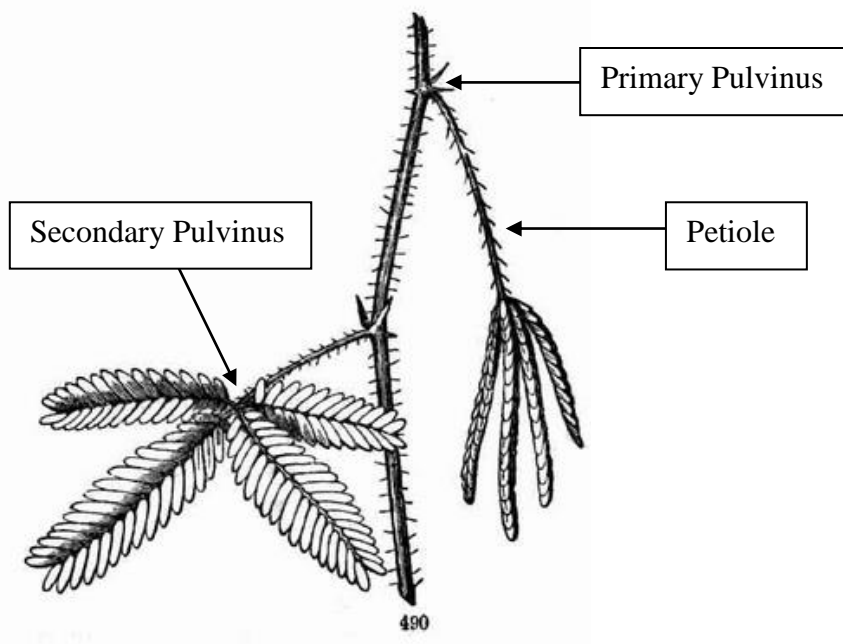


Figure A1. Anatomy of Mimosa Pudica

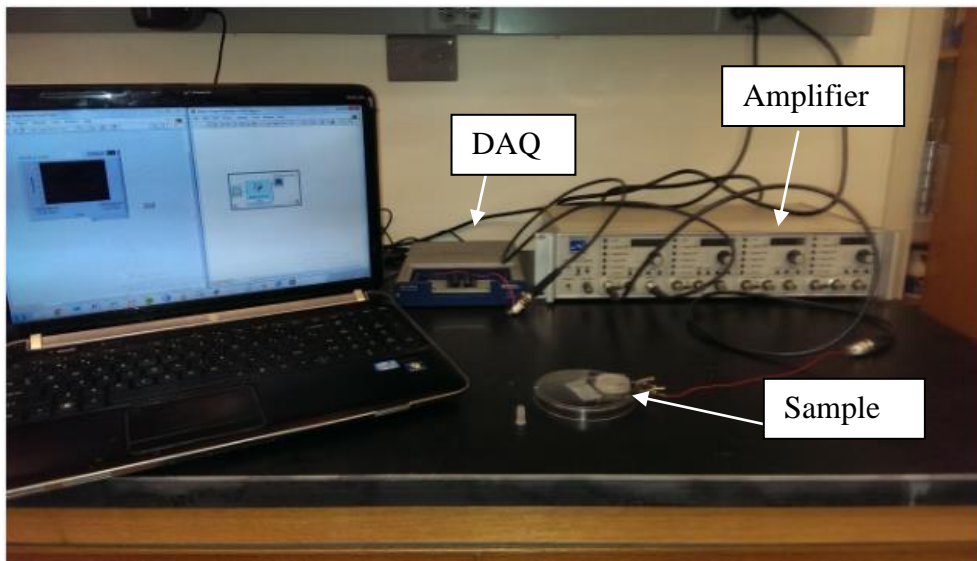
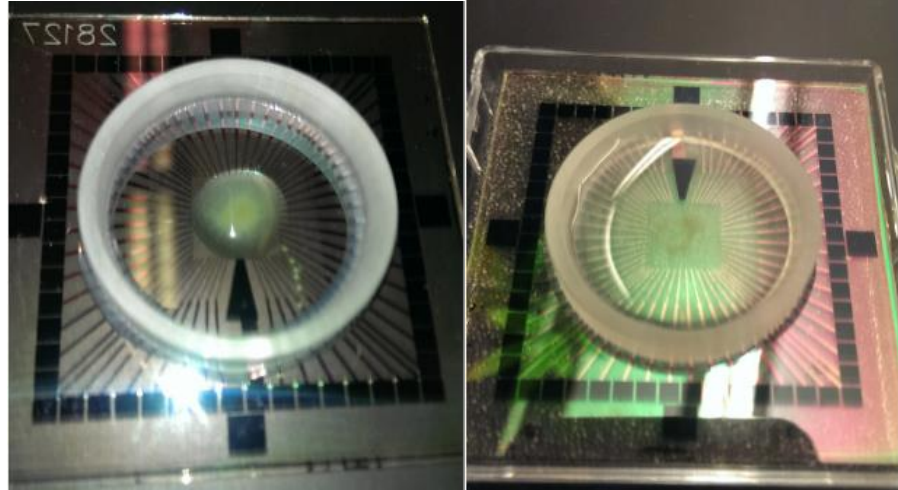
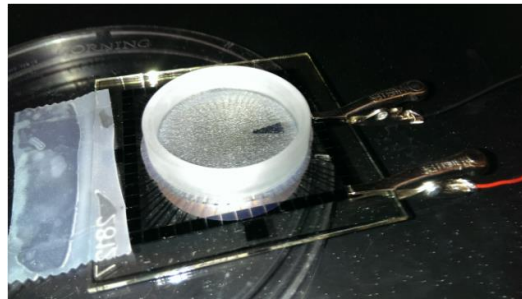


Figure A2. Electrophysiology Testing Stage



a)

b)

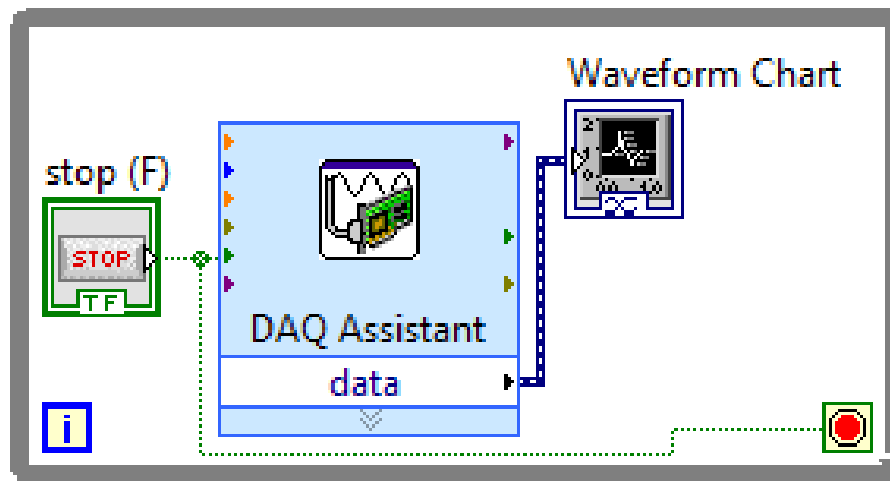
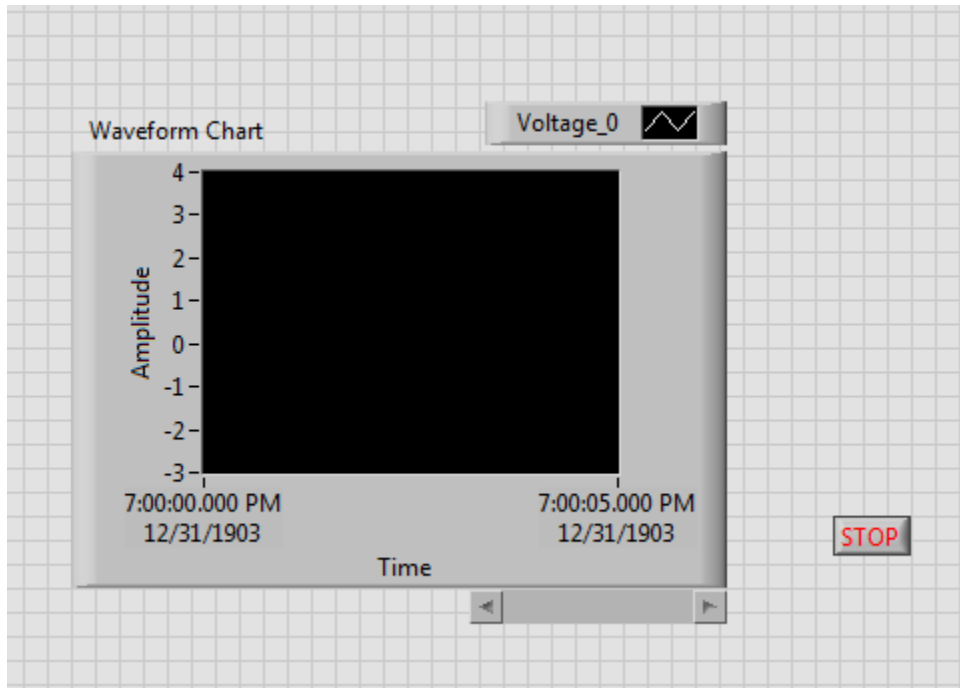


c)

Figure 7. MEA with Protoplasts a) in isolated droplet b) after agar has been added c) after solification

## Appendix B: Code

### Code B1: LabVIEW Panels for Data Acquisition





## Code B2: Matlab Code for Data Analysis (File name chosen is a random data set)

```
%Clear previous variables and screen
clc
clear

%Define file
filename = '4-16-15 CompleteChronic_HP75_LP10k_G3.xlsx';
%Identify excel data of interest
range = 'D2:D5001';
%Read the data of interest
data = xlsread(filename, range);
y = data';
%Prepare to take the FFT of y
L = length(y);
NFFT = 2^nextpow2(L);
%Resample the data to a multiple of 60
y_resampled = resample(y,6,10);
%Take the FFT of y
Y = fft(y_resampled,NFFT)/L;
Fs = 600;
f = Fs/2*linspace(0,1,NFFT/2+1);

%Define the notching comb filter parameters
N = 10; % Order
Q = 3; % Q-factor
Apass = 1; % Bandwidth Attenuation

BW = 2*Fs/2/10/Q;

% Calculate the coefficients using the IIRCOMB function.
[b, a] = iircomb(N, BW/(Fs/2), Apass);
Hd = dfilt.df2(b, a);

%Filter data
y_filtered = filter(Hd,y_resampled);
Y_filtered = fft(y_filtered,NFFT)/L;

% Plot single-sided amplitude spectrum and time signal before and after
% filtering
subplot(2,2,1)
plot(f,2*abs(Y(1:NFFT/2+1)))
title('Single-Sided Amplitude Spectrum of y(t)')
xlabel('Frequency (Hz)')
ylabel('|Y(f)|')
subplot(2,2,2)
plot(linspace(0,5,3000),y_resampled)
title('Time Domain of y(t)')
xlabel('Time (s)')
ylabel('Voltage (V)')
subplot(2,2,3)
plot(f,2*abs(Y_filtered(1:NFFT/2+1)))
```

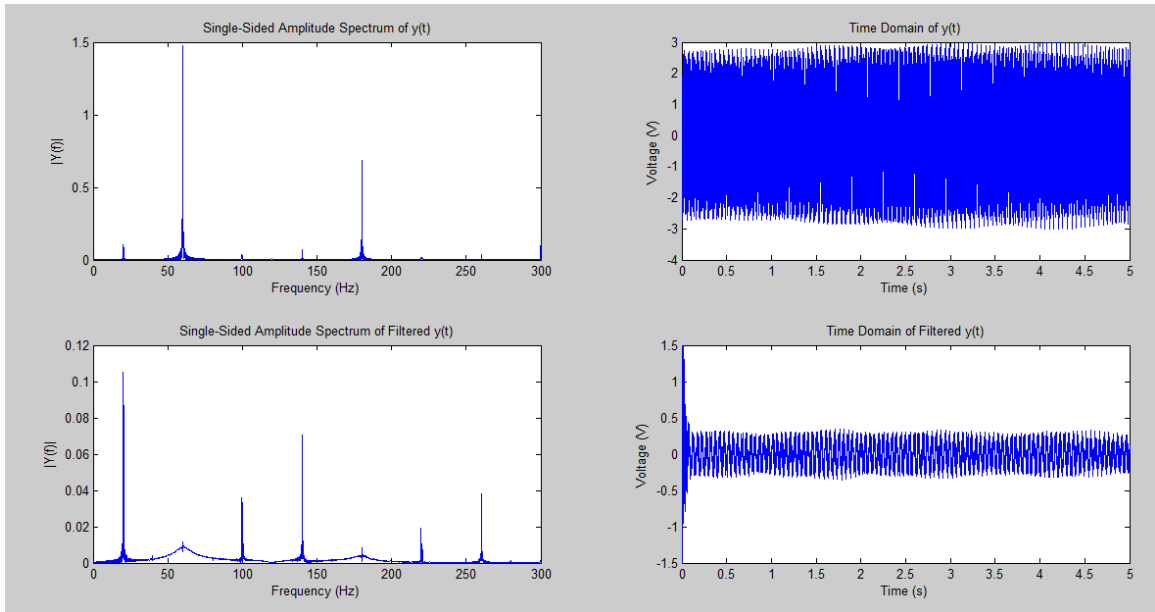
```
title('Single-Sided Amplitude Spectrum of Filtered y(t)')
xlabel('Frequency (Hz)')
ylabel('|Y(f)|')
subplot(2,2,4)
plot(linspace(0,5,3000),y_filtered)
title('Time Domain of Filtered y(t)')
xlabel('Time (s)')
ylabel('Voltage (V)')
ylim([-1.5 1.5])
```

## Appendix C: Bulk Data

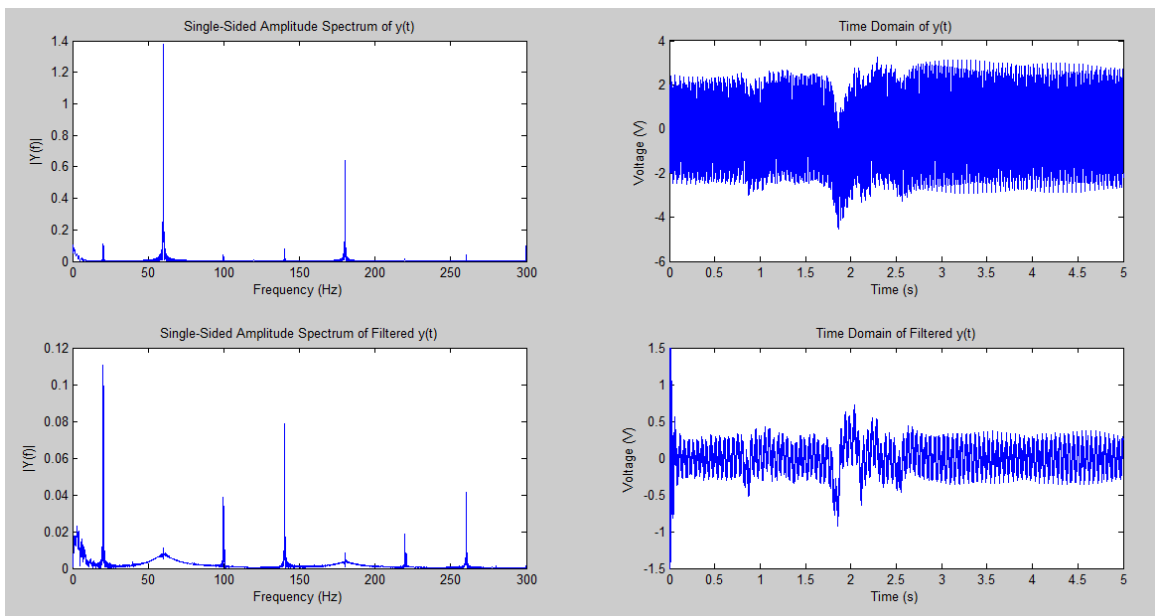
\*All data without other specifications have a LPF setting of 10kHz, HPF setting of

0.1Hz, and a gain factor of 400

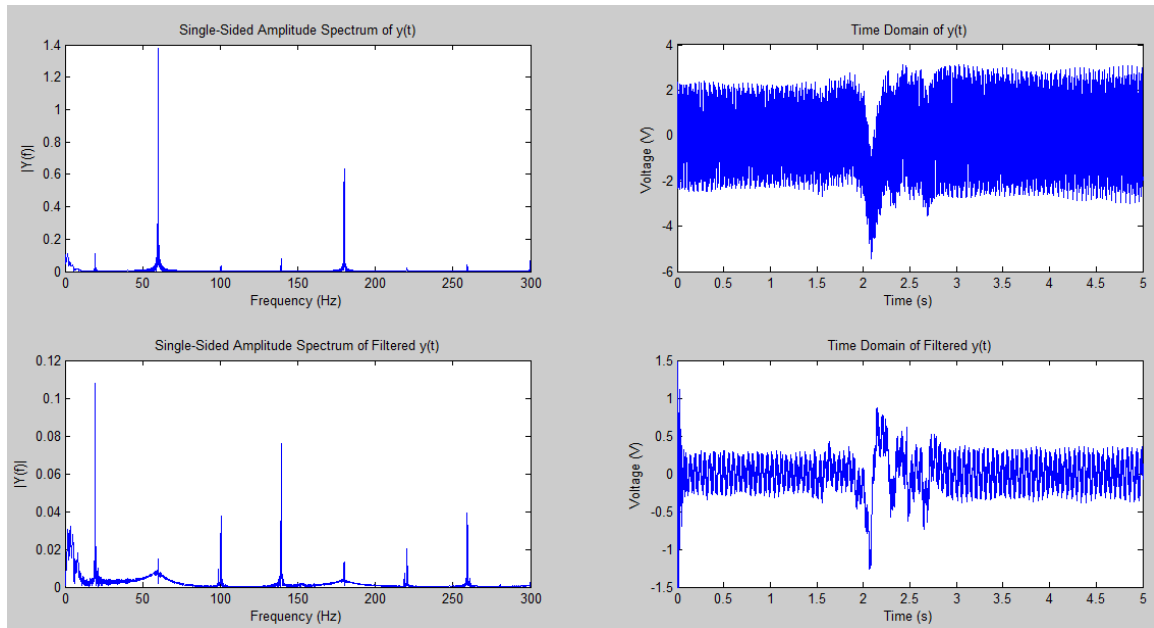
### 4/11/15 Control with Cells



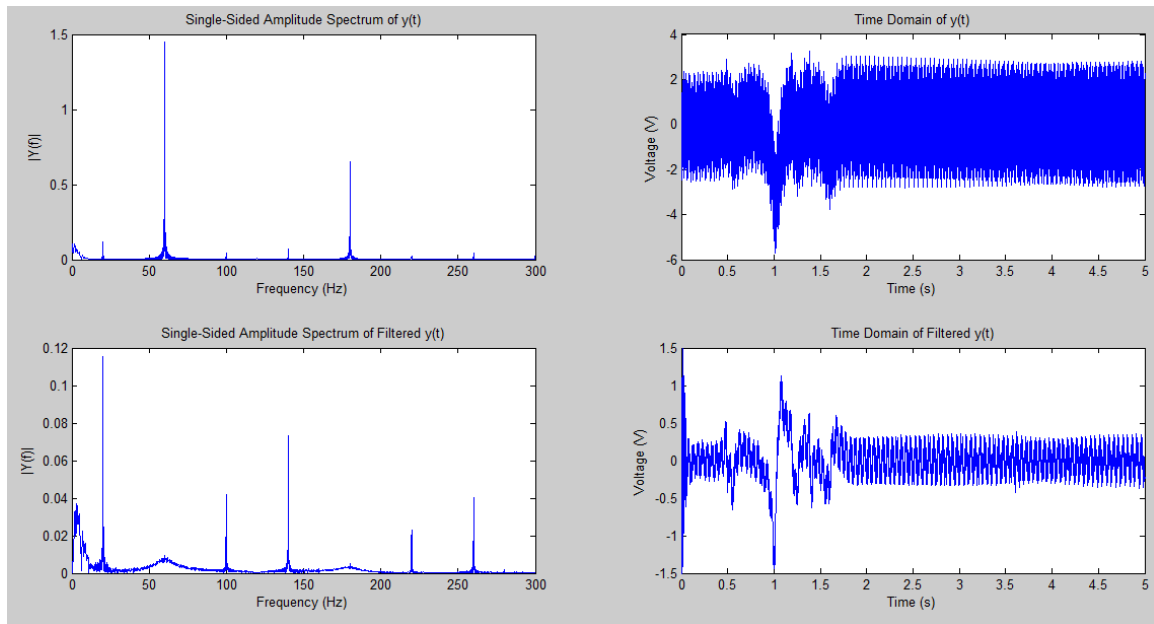
### 4/11/15 Acute Trial 1 Data



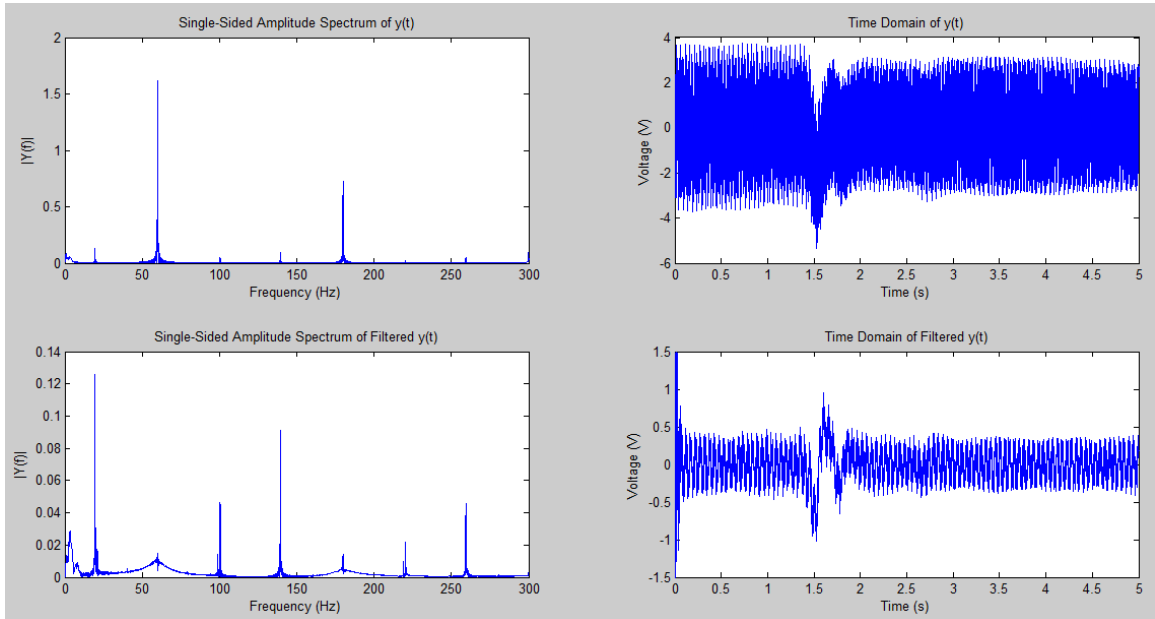
### 4/11/15 Acute Trial 2



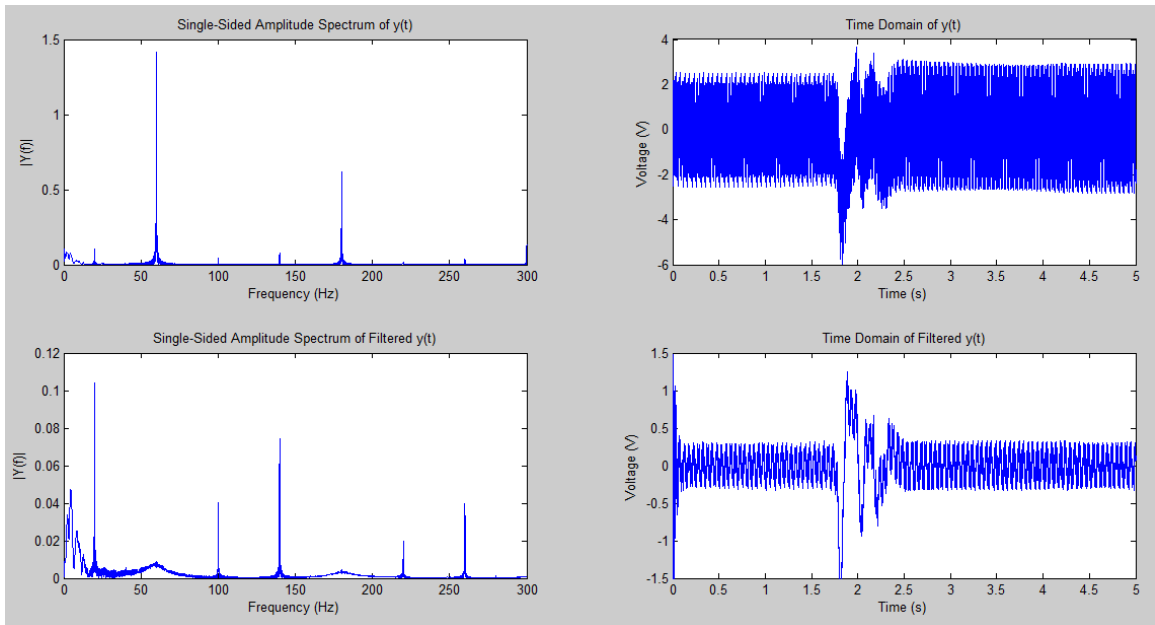
### 4/11/15 Acute Trial 3



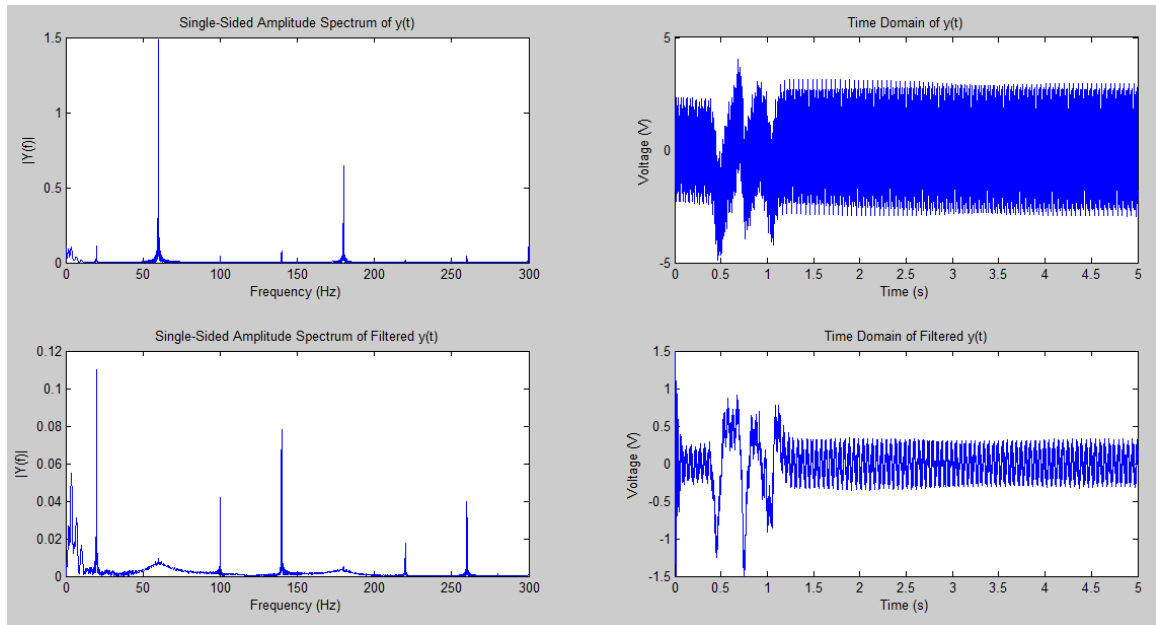
## 4/11/15 Chronic Trial 1



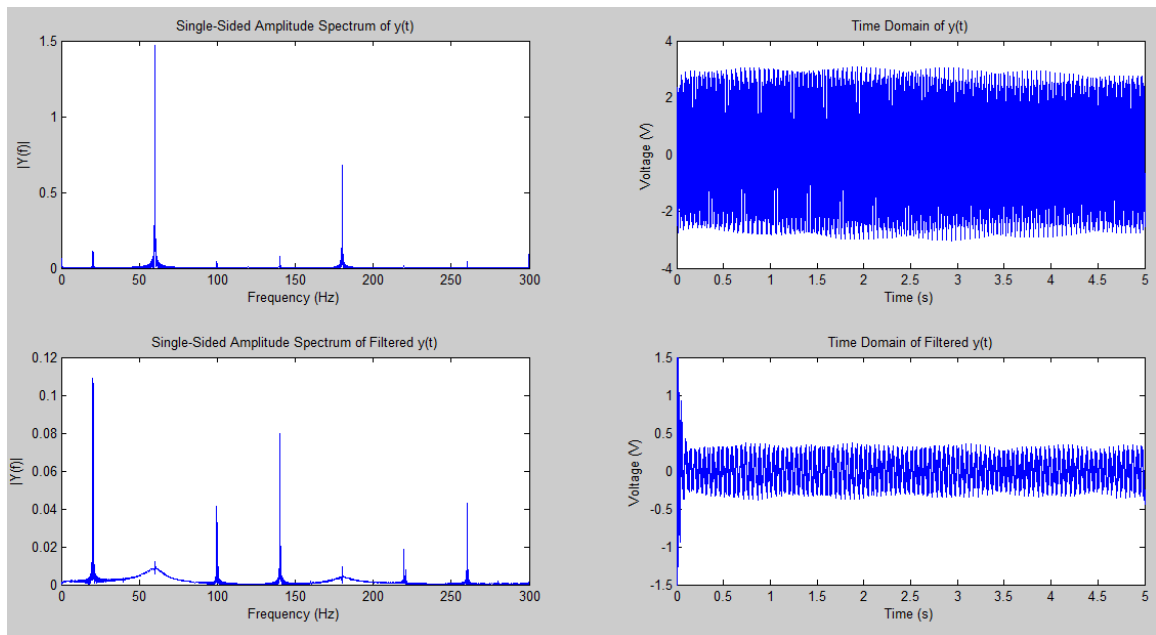
## 4/11/15 Chronic Trial 2



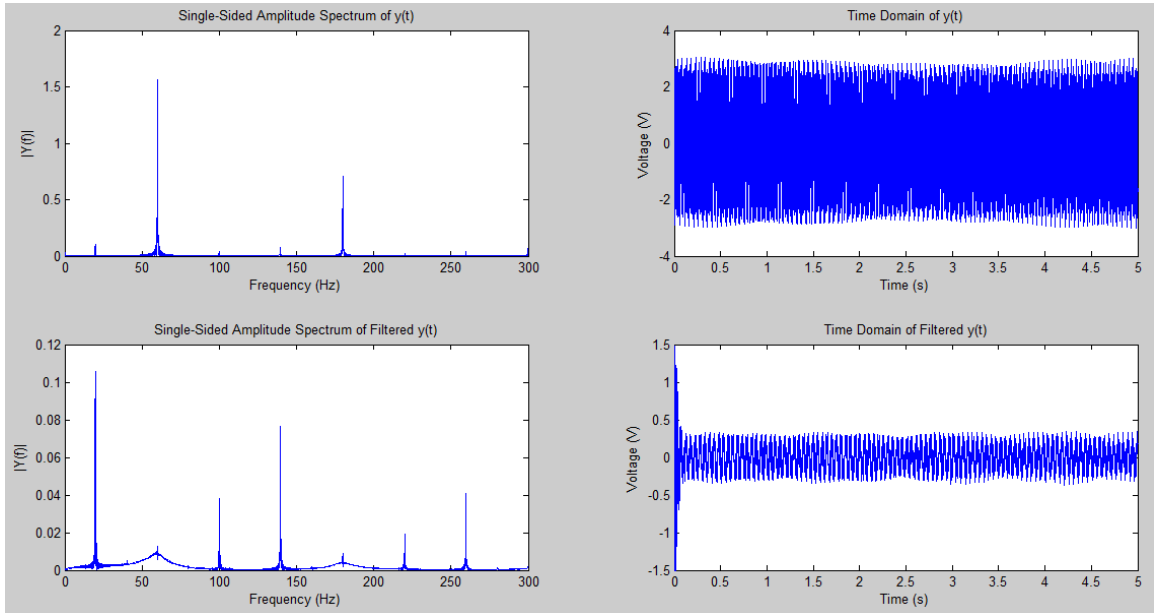
### 4/11/15 Chronic Trial 3



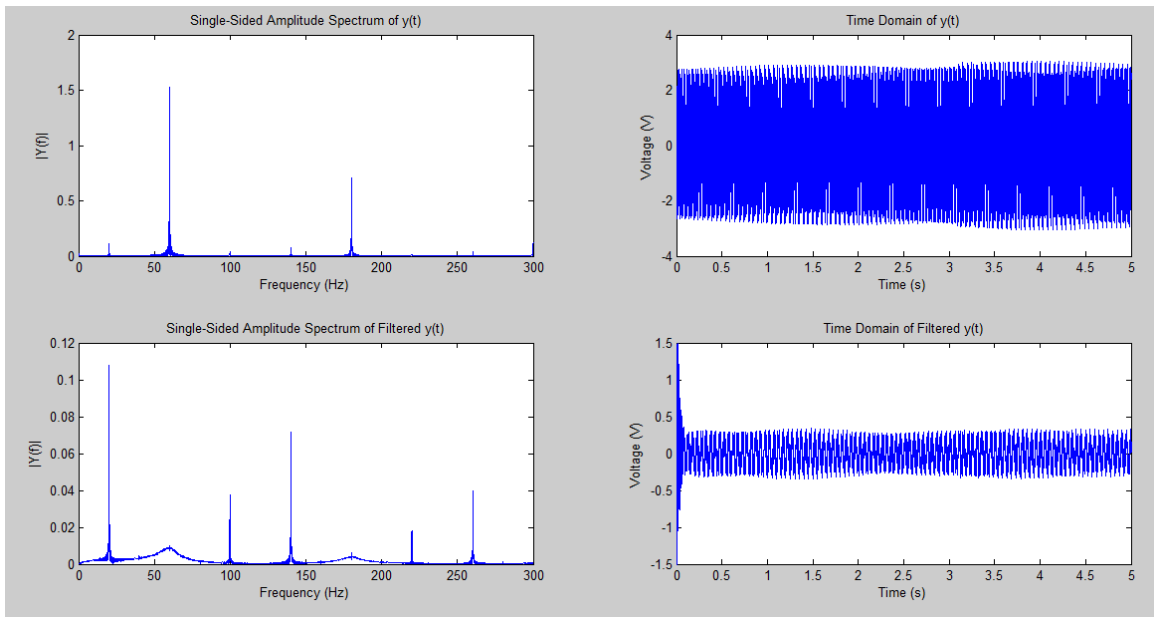
### 4/11/15 Set Trial 1



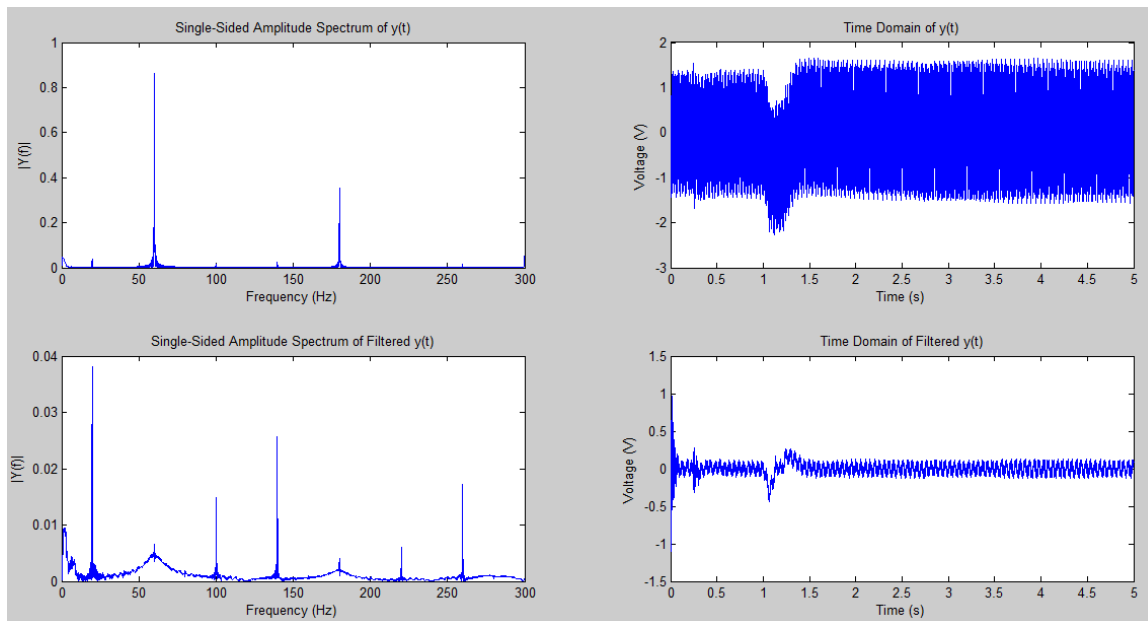
### 4/11/15 Set Trial 2



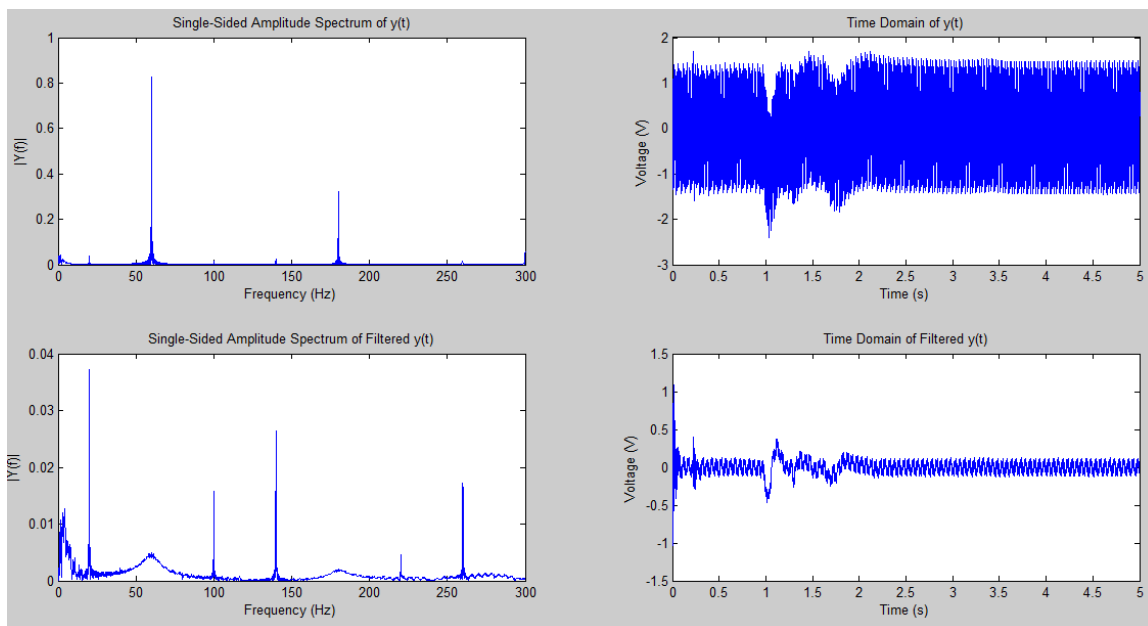
### 4/11/15 Set Trial 3



### 4/12/15 No Cell Acute Trial 1

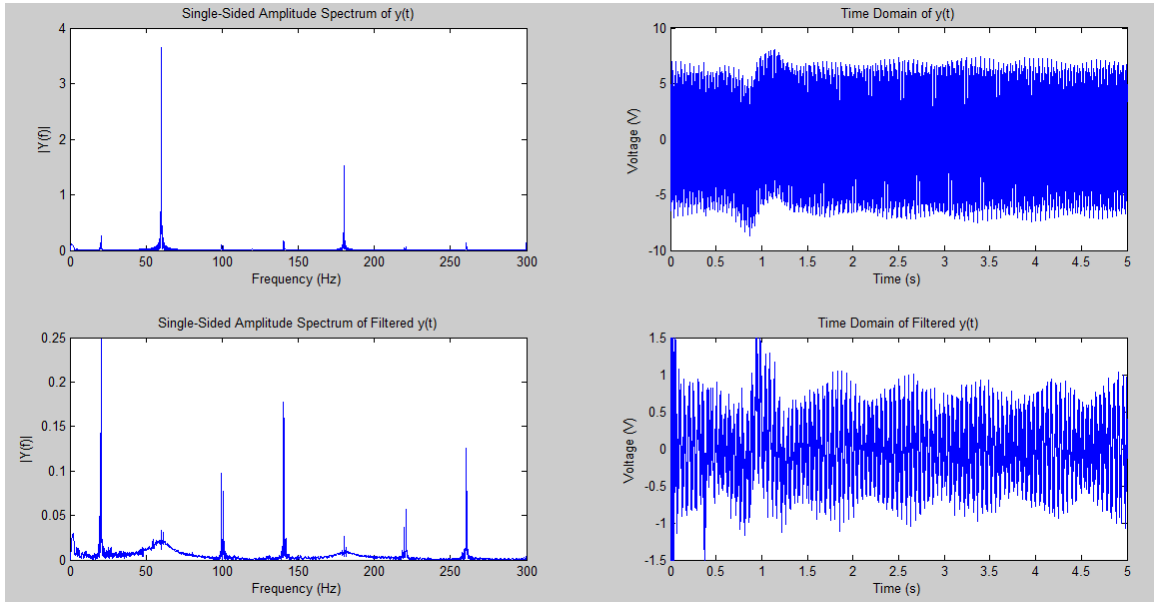


### 4/12/15 No Cell Acute Trial 2

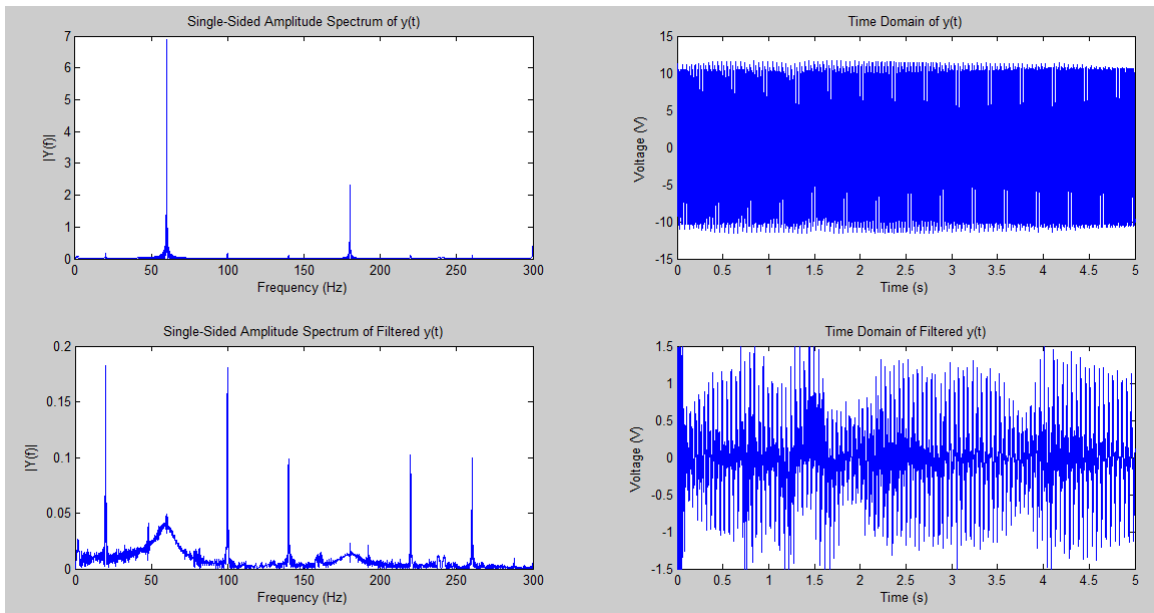




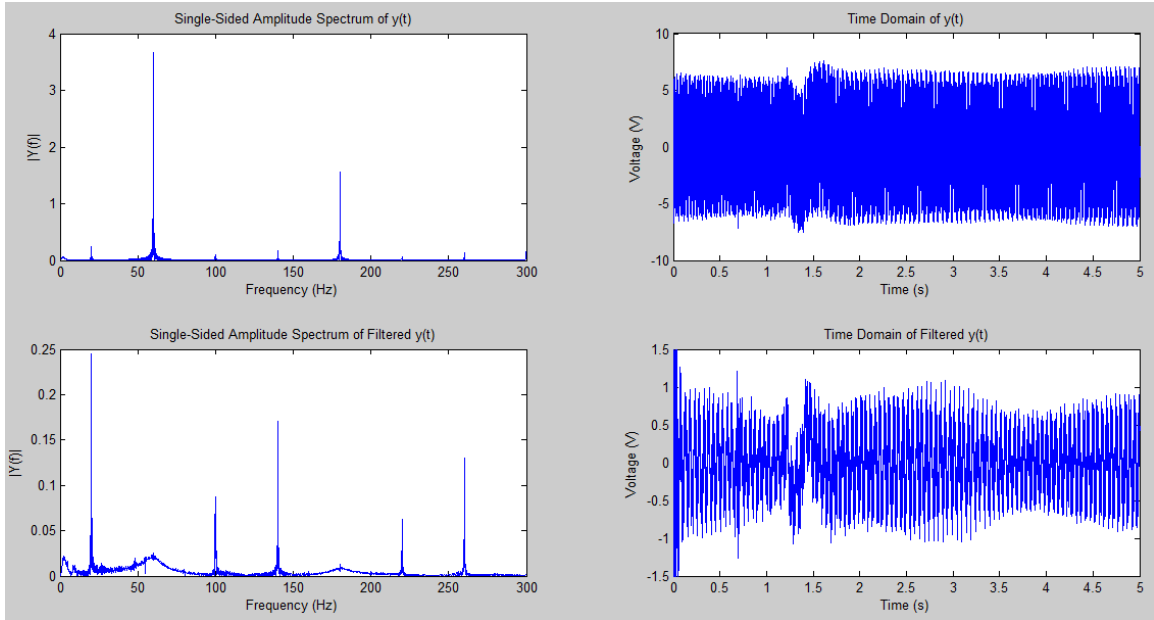
4/12/15 No Cell Chronic Trial 1 (LPF = 10kHz; HPF = 1Hz; Gain = 2k)



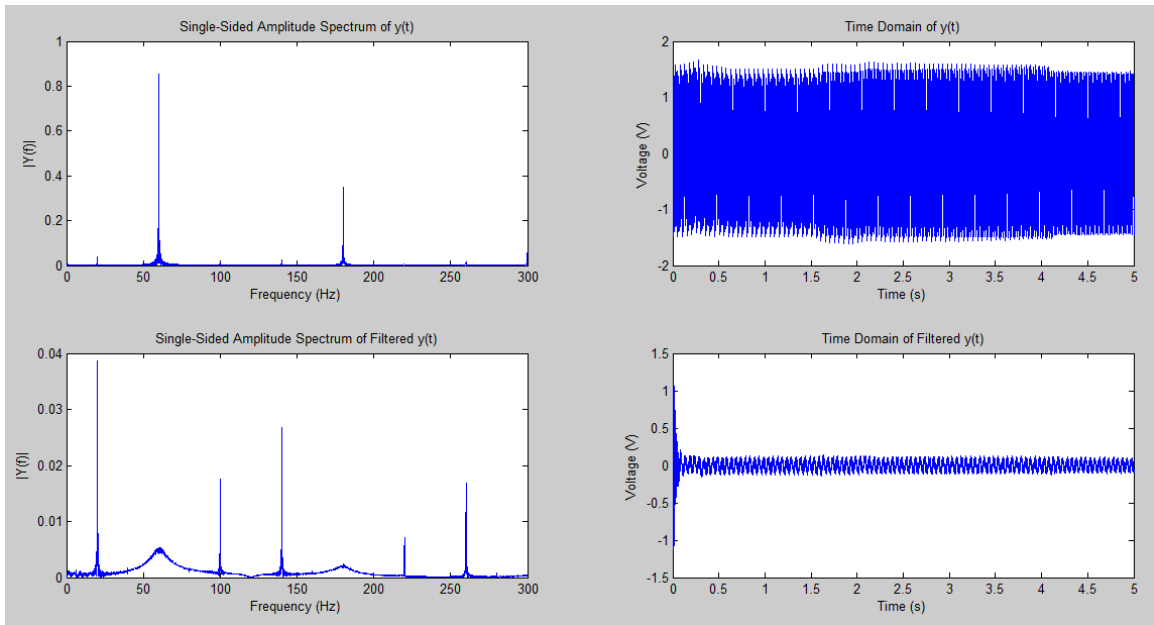
4/12/15 No Cell Chronic Trial 2 (LPF = 10kHz; HPF = 1Hz; Gain = 5k)



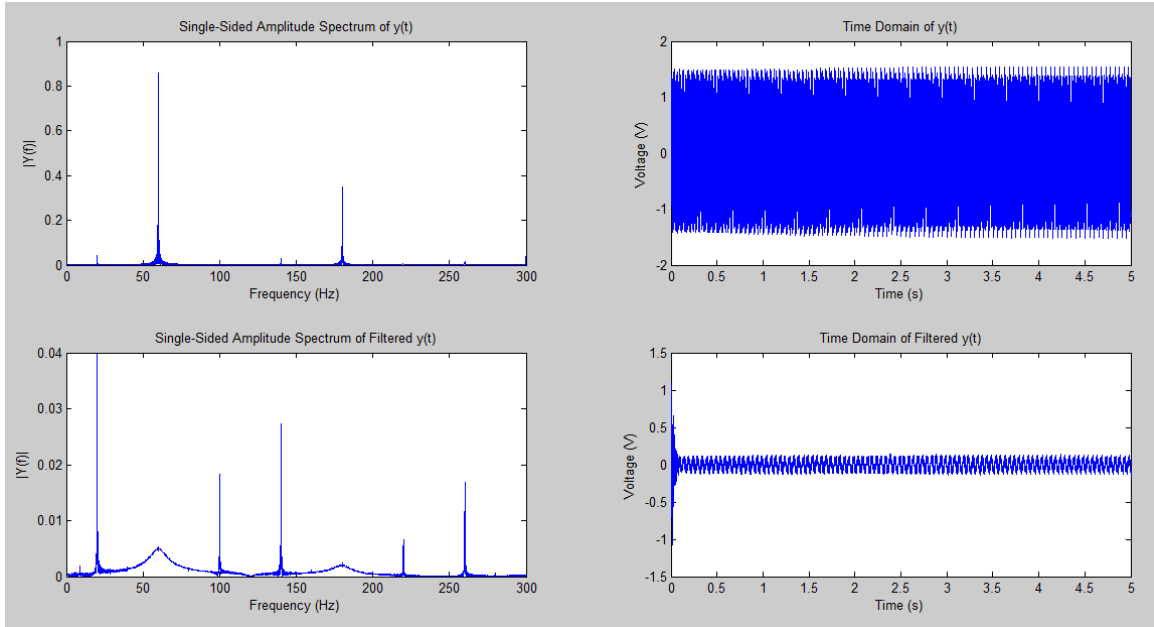
4/12/15 No Cell Chronic Trial 3 (LPF = 10kHz; HPF = 3Hz; Gain = 2k)



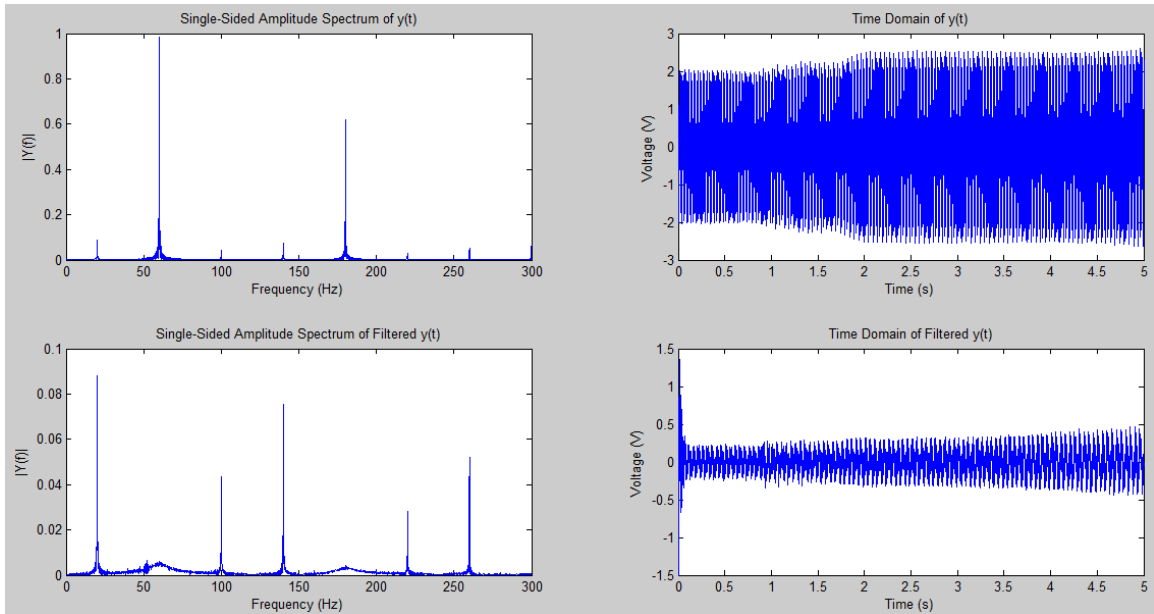
4/12/15 Control with no Cells Data



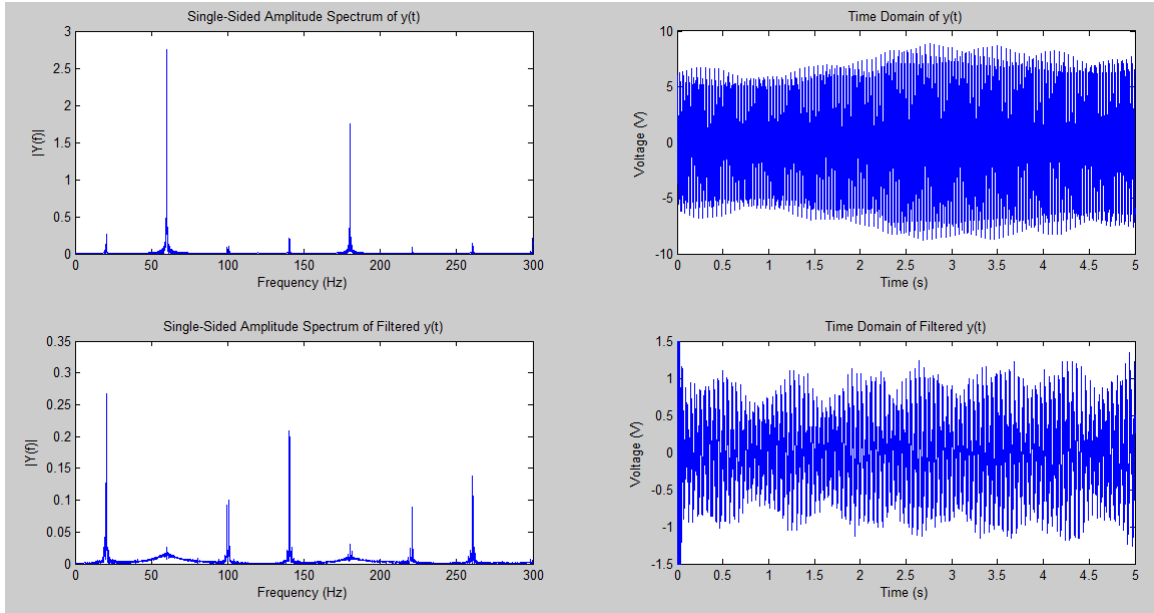
### 4/12/15 No Cell Set Trial 1 Data



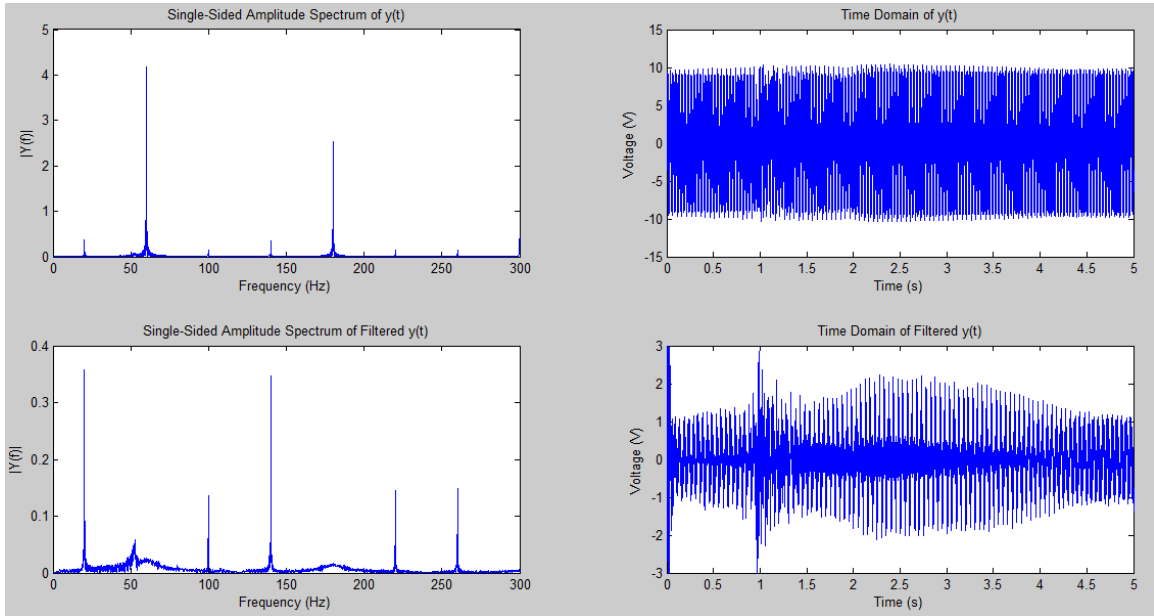
### 4/16/15 Acute Trial 1 (LPF = 10kHz; HPF = 75Hz; Gain = 1k)



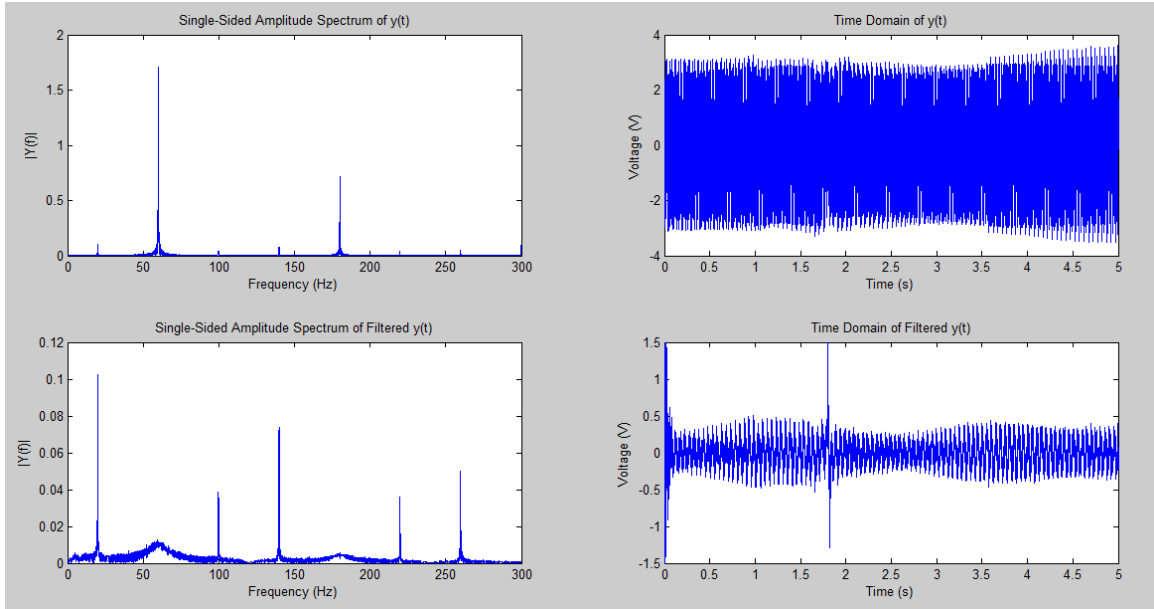
4/16/15 Acute Trial 2 (LPF = 10kHz; HPF = 75Hz; Gain = 3k)



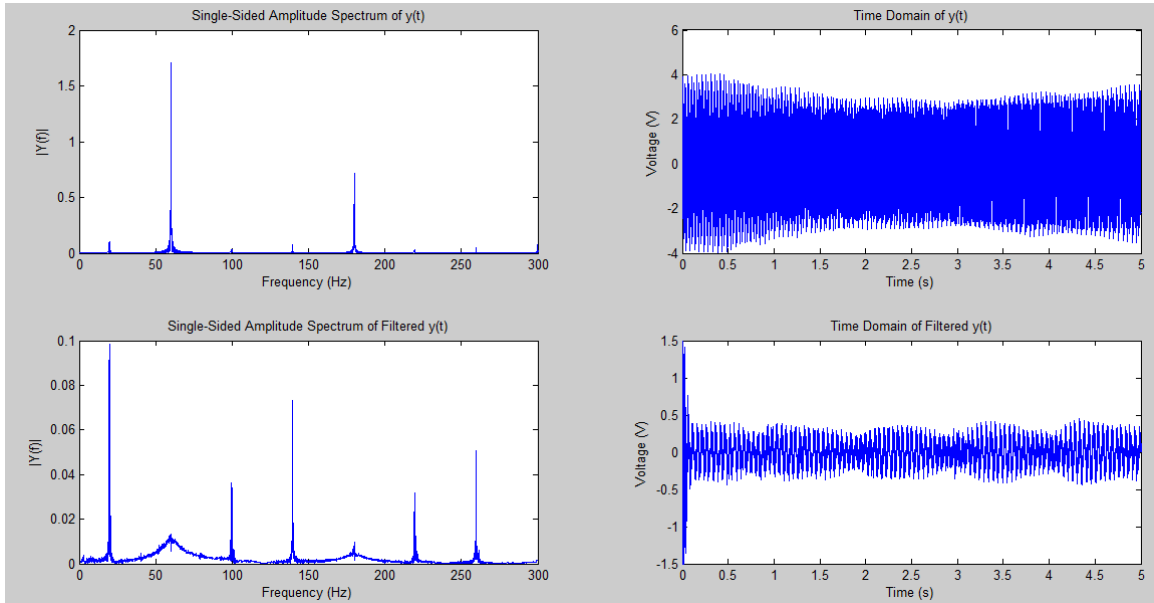
4/16/15 Acute Trial 3 (LPF = 10kHz; HPF = 75Hz; Gain = 5k)



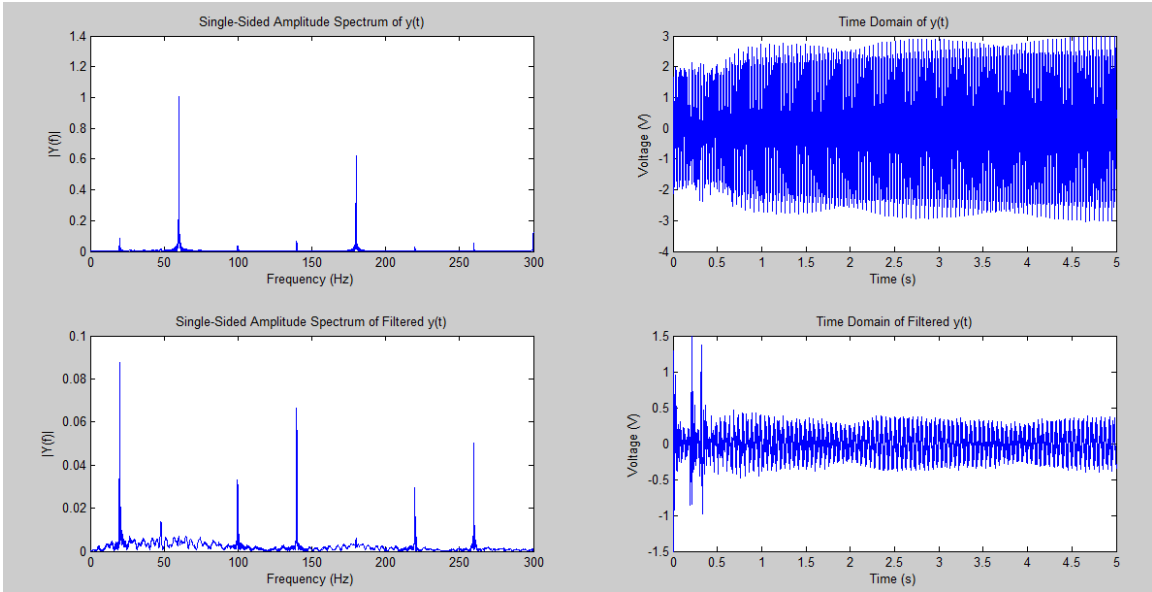
4/16/15 Chronic Trial 1 (LPF = 10kHz; HPF = 1Hz; Gain = 1k)



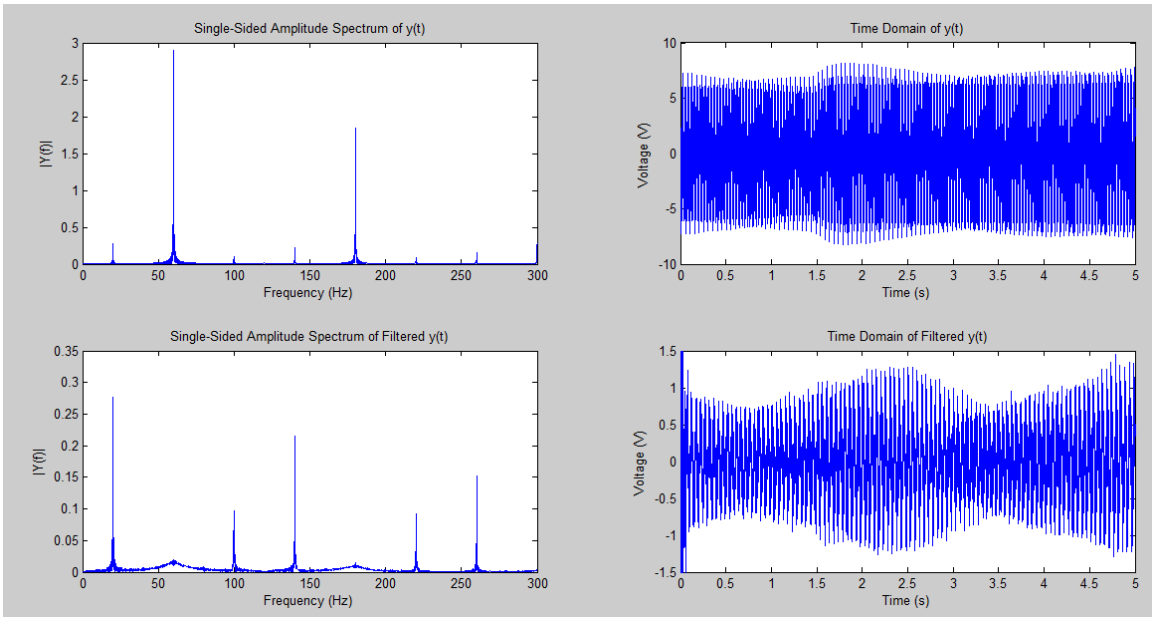
4/16/15 Chronic Trial 2 (LPF = 10kHz; HPF = 1Hz; Gain = 1k)



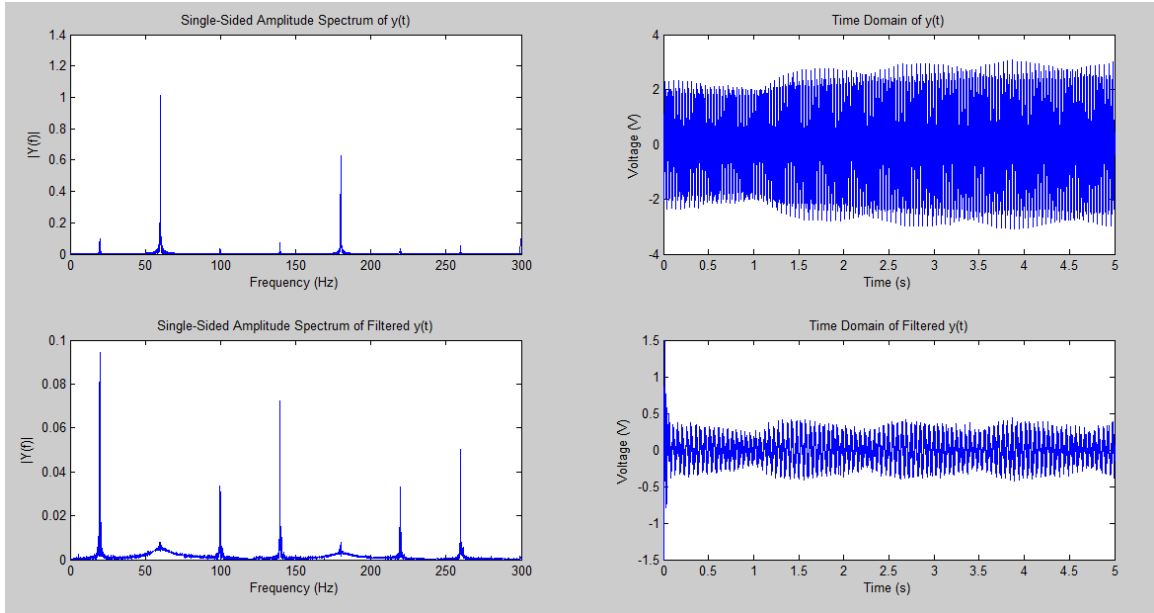
4/16/15 Chronic Trial 3 (LPF = 10kHz; HPF = 75Hz; Gain = 1k)



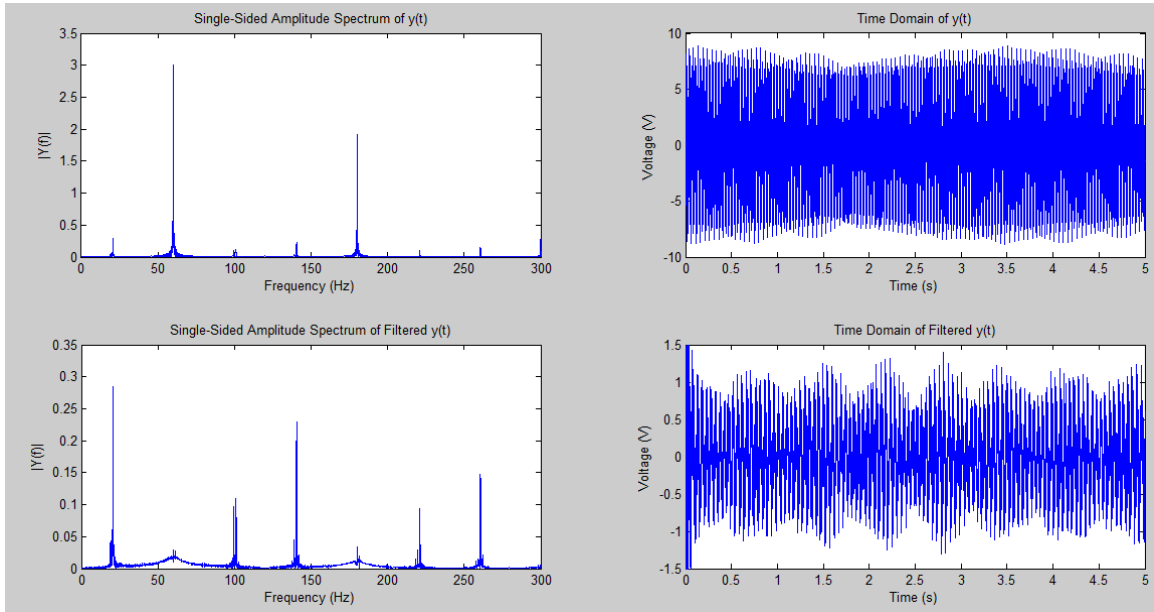
4/16/15 Chronic Trial 4 (LPF = 10kHz; HPF = 75Hz; Gain = 3k)



4/16/15 Chronic Trial 5 (LPF = 20kHz; HPF = 75Hz; Gain = 1k)



4/16/15 Control with Cells (LPF = 10kHz; HPF = 75Hz; Gain = 3k)



4/16/15 Set Trial 1 (LPF = 10kHz; HPF = 75Hz; Gain = 3k)

